

## Accepted Manuscript

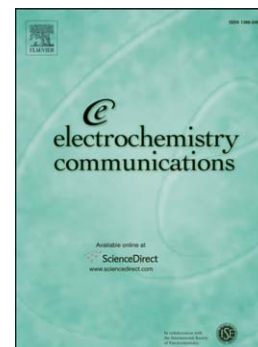
PdPt alloy nanocubes as electrocatalysts for oxygen reduction reaction in acid media

Kristel Jukk, Nadezda Kongi, Kaido Tammeveski, Jose Solla-Gullón, Juan M. Feliu

PII: S1388-2481(15)00098-3  
DOI: doi: [10.1016/j.elecom.2015.04.001](https://doi.org/10.1016/j.elecom.2015.04.001)  
Reference: ELECOM 5423

To appear in: *Electrochemistry Communications*

Received date: 17 March 2015  
Revised date: 31 March 2015  
Accepted date: 1 April 2015



Please cite this article as: Kristel Jukk, Nadezda Kongi, Kaido Tammeveski, Jose Solla-Gullón, Juan M. Feliu, PdPt alloy nanocubes as electrocatalysts for oxygen reduction reaction in acid media, *Electrochemistry Communications* (2015), doi: [10.1016/j.elecom.2015.04.001](https://doi.org/10.1016/j.elecom.2015.04.001)

This is a PDF file of an unedited manuscript that has been accepted for publication. As a service to our customers we are providing this early version of the manuscript. The manuscript will undergo copyediting, typesetting, and review of the resulting proof before it is published in its final form. Please note that during the production process errors may be discovered which could affect the content, and all legal disclaimers that apply to the journal pertain.

## PdPt alloy nanocubes as electrocatalysts for oxygen reduction reaction in acid media

Kristel Jukk<sup>a</sup>, Nadezda Kongi<sup>a</sup>, Kaido Tammeveski<sup>a,\*</sup>, Jose Solla-Gullón<sup>b</sup>, Juan M. Feliu<sup>b</sup>

<sup>a</sup>*Institute of Chemistry, University of Tartu, Ravila 14<sup>a</sup>, 50411 Tartu, Estonia*

<sup>b</sup>*Instituto de Electroquímica, Universidad de Alicante, Apartado 99, 03080 Alicante, Spain*

### Abstract

In this work, PdPt alloy nanocubes with different metal ratios were synthesised in the presence of polyvinylpyrrolidone (PVP). The surface morphology of the PdPt samples was characterised by transmission electron microscopy (TEM). TEM images showed that PdPt nanoparticles were cubic-shaped and the average size of the cubes was about 8-10 nm. Their electrocatalytic activity towards the oxygen reduction reaction (ORR) was studied in 0.5 M H<sub>2</sub>SO<sub>4</sub> using the rotating disk electrode method. All the alloyed catalysts showed enhanced electrocatalytic activity for ORR as compared to the monometallic cubic Pd nanoparticles. Half-wave potential values for PdPt catalysts were comparable with that of Pt nanocubes. From the alloyed catalysts Pd<sub>36</sub>Pt<sub>64</sub> exhibited the highest specific activity, which was only slightly lower than that of cubic Pt nanoparticles. The Koutecky-Levich analysis revealed that the reduction of oxygen proceeded via 4-electron pathway on all the electrocatalysts studied.

**Keywords:** PdPt alloy nanoparticles; Oxygen reduction; Electrocatalysis; Shape-controlled nanocubes; Bimetallic catalysts.

---

\*Corresponding author. Tel.: +372-7375168; fax: +372-7375181  
E-mail address: [kaido.tammeveski@ut.ee](mailto:kaido.tammeveski@ut.ee) (K. Tammeveski)

## 1. Introduction

Platinum-based catalysts are the best electrocatalysts for oxygen reduction reaction (ORR) in fuel cells [1,2]. However, because of the high price and limited supply of Pt, numerous researches have focused on finding a way to reduce its amount in the catalysts. One way to decrease Pt loading is to replace it partially by other metals. However, the change of metallic composition not only decreases the amount of Pt, but also modifies the crystallographic and electronic structures of Pt, which can affect the binding energy between Pt and oxygen [3]. Palladium is a promising substitute due to the similar properties to the Pt (same group of the periodic table, similar atomic size and crystalline structure) [4].

Catalytic properties of alloy nanostructures are significantly influenced by the shape, size, composition and surface structure [5-7]. Controlling the shape and facets of nanocrystals is an effective way to enhance the performance in catalytic reactions [5-8]. Recently, several researches have been aimed towards the electrocatalytic studies of shape-controlled Pt-Pd alloy nanocrystals [3,5-15]. Hong et al. synthesised Pd-Pt alloys with hollow nanostructures and studied the electrocatalysis of the ORR on these materials [3]. They found that the electrocatalytic activity is highly dependent on the nanoparticle's morphology and reported highest ORR activity with hollow nanocrystals. Lim and co-workers studied oxygen reduction on Pd-Pt bimetallic nanodendrites, which were 2.5 times more active than commercial Pt/C catalyst [9]. The higher activity was attributed to the favourable adsorption of O<sub>2</sub> molecules on the stepped surfaces. Gong et al. showed that the ORR activity of Pt monolayer on Pd tetrahedral nanocrystals depends on the removal of surfactants from the catalyst surface [10]. Zheng and co-workers explored the electroreduction of oxygen on PtPd nanoflowers and stated that these catalysts exhibited improved electrocatalytic activity for ORR [11]. Lee et al. studied the reduction of O<sub>2</sub> on Pt-coated Pd nanocubes in alkaline solution and concluded that the core-shell nanocubes showed 2.6 times higher specific activity than Pt nanoparticles [14].

To our knowledge, the literature about oxygen reduction on PdPt alloy nanocubes is scarce. In this work, the reduction of oxygen on PdPt alloy nanocubes synthesised in the presence of PVP was investigated using a rotating disk electrode. Different Pd-to-Pt ratios were used and the electrocatalytic activity of PdPt catalysts for ORR was compared with that of cubic Pd and Pt nanoparticles.

## 2. Experimental

PdPt alloy nanocubes were synthesised using a similar methodology to that described elsewhere [16]. Briefly, 20 mM potassium tetrachloropalladate (>99.99%, Sigma-Aldrich), 20 mM potassium tetrachloroplatinate (>99.99%, Sigma-Aldrich), 75 mg of sodium iodide ( $\geq$ 99.99%, Sigma-Aldrich) and 160 mg of poly(vinylpyrrolidone) (PVP, MW $\approx$ 55000, Sigma-Aldrich) were mixed together with 10 mL N,N-dimethylformamide (Sigma-Aldrich) in a glass vial and the mixture was sonicated for 2 min. The resulting homogeneous mixture was capped, transferred to an oven and heated at 130 °C for 3 h before cooling down to room temperature. The colloidal products were collected by centrifugation and washed several times with an ethanol-acetone mixture and finally stored in ultrapure water. In order to synthesise PdPt alloy nanocubes with different composition, the amount of  $K_2PdCl_4$  and  $K_2PtCl_4$  was accordingly varied. The nominal PdPt alloy compositions were 34/66, 50/50 and 66/34. The surface morphology and composition of PdPt alloy nanocubes was characterised using a transmission electron microscope (JEOL, JEM-2010 working at 200 kV) equipped with an X-ray detector OXFORD INCA Energy TEM 100 for microanalysis (EDX). The TEM samples were prepared by placing an aliquot of diluted ethanol/acetone dispersions onto a Formvar-covered copper grid and allowing the solvent to evaporate in air. For comparison purposes, Pd and Pt nanocubes were also checked. Pd nanocubes were synthesised by CTAB method [17,18] and Pt nanocubes by microemulsion method [19]. The average particle size

for Pd nanocubes was 20-25 nm and for Pt nanocubes 10 nm. Glassy carbon (GC) electrodes with geometric area ( $A$ ) of  $0.071 \text{ cm}^2$  were used in this work.

Electrochemical experiments were conducted in a three-electrode cell in  $0.5 \text{ M H}_2\text{SO}_4$  solution (Suprapur, Merck) using an Autolab potentiostat/galvanostat PGSTAT30 (Eco Chemie B.V.). The electrolyte was saturated with  $\text{O}_2$  (99.999%, AGA) or Ar (99.999%, AGA). A Pt wire was used as a counter electrode and all the potentials are referred to the reversible hydrogen electrode (RHE). Cyclic voltammetry (CV) experiments were performed in Ar-saturated solutions at a potential scan rate ( $\nu$ ) of  $50 \text{ mV s}^{-1}$ . CO adsorption-stripping was used as a final cleaning step of the catalyst surface. The electrode potential was held at  $0.05 \text{ V}$  and CO gas was introduced into the electrochemical cell. After one min. of constant bubbling throughout the electrolyte, CO was replaced by Ar for 30 min., still at  $0.05 \text{ V}$ , to remove the dissolved CO from the solution. For CV and CO stripping experiments the current densities were calculated per real surface area of the catalysts. The charge corresponding to  $\text{H}_{\text{upd}}$  desorption was used for the calculation of the real area ( $A_r$ ) of the PdPt alloy, Pd and Pt cubes ( $\text{H}_{\text{upd}}(\text{Pt}) = 210 \mu\text{C cm}^{-2}$  [20] and  $\text{H}_{\text{upd}}(\text{Pd}) = 212 \mu\text{C cm}^{-2}$  [21]).

### 3. Results and discussion

#### 3.1. TEM/EDX characterisation of PdPt catalysts

Representative TEM images of the PdPt nanocubes are shown in Fig 1. In all cases, a preferential cubic particle shape is clearly identified. The average particle size was  $8.6 \pm 0.9$ ,  $9.4 \pm 1.4$  and  $10.4 \pm 1.2 \text{ nm}$  corresponding to  $\text{Pd}_{34}\text{Pt}_{66}$ ,  $\text{Pd}_{50}\text{Pt}_{50}$  and  $\text{Pd}_{66}\text{Pt}_{34}$  samples, respectively. The EDX analysis revealed that the atomic composition of the synthesised PdPt alloy nanocubes was in good agreement with the nominal ones and Pd:Pt ratios of 36:64, 54:46 and 72:28 were obtained.

### 3.2. CO stripping and CV experiments

The CO adsorption and stripping procedure was used to electrochemically clean the surface of PdPt alloy nanocubes without changing their nanostructure. Typical CO-stripping behaviour of PdPt catalysts is shown in Fig. 2a. Well-defined CO electro-oxidation peaks can be observed at 0.83, 0.87 and 0.93 V for Pd<sub>36</sub>Pt<sub>64</sub>, Pd<sub>54</sub>Pt<sub>46</sub> and Pd<sub>72</sub>Pt<sub>28</sub> nanocubes, respectively. It can be seen that the CO-oxidation peak shifts positive with increasing the amount of Pd. This is in good agreement with previous observations [20]. The CO-oxidation peaks for pure Pd and Pt nanocubes are centred at 0.94 and 0.77 V, respectively.

Representative CVs recorded after the CO-stripping experiments are shown in Fig. 2b. The CV responses showed improvement in surface cleanness compared with those initially measured. Better defined peaks in the hydrogen adsorption/desorption region are in evidence. The real surface areas of the PdPt electrocatalysts were determined by charge integration under the hydrogen desorption peaks (see Table 1).

### 3.3. Oxygen reduction on PdPt catalysts

The electroreduction of oxygen on PdPt alloy nanocubes was studied in O<sub>2</sub>-saturated 0.5 M H<sub>2</sub>SO<sub>4</sub> solution using the RDE method. The representative ORR polarisation curves for the Pd<sub>54</sub>Pt<sub>46</sub>-catalyst modified GC electrode are shown in Fig. 3a, the background currents were recorded at 10 mV s<sup>-1</sup> between 0.05 and 1.0 V in Ar-saturated electrolyte and were subtracted from these data. Only the positive-going potential scans are presented and further analysed. For all the PdPt catalysts the ORR polarisation curves were single-waved and well-defined diffusion-limited current plateaus were observed.

The number of electrons transferred per O<sub>2</sub> molecule (*n*) was calculated from the RDE data using the Koutecky-Levich (K-L) equation [22]:

$$\frac{1}{j} = \frac{1}{j_k} + \frac{1}{j_d} = -\frac{1}{nFkC_{O_2}^b} - \frac{1}{0.62nFD_{O_2}^{2/3}v^{-1/6}C_{O_2}^b\omega^{1/2}} \quad (1)$$

where  $j$  is the measured current density,  $j_k$  and  $j_d$  are the kinetic and diffusion-limited current densities, respectively,  $k$  is the rate constant for ORR,  $F$  is the Faraday constant (96,485 C mol<sup>-1</sup>),  $\omega$  is the rotation rate,  $C_{O_2}^b$  is the concentration of O<sub>2</sub> in the bulk ( $1.13 \times 10^{-6}$  mol cm<sup>-3</sup>) [23],  $D_{O_2}$  is the diffusion coefficient of O<sub>2</sub> ( $1.8 \times 10^{-5}$  cm<sup>2</sup> s<sup>-1</sup>) [23] and  $\nu$  is the kinematic viscosity of the solution (0.01 cm<sup>2</sup> s<sup>-1</sup>) [24]. Fig. 3b presents the K-L plots for Pd<sub>54</sub>Pt<sub>46</sub>-catalyst. The value of  $n$  was close to four for all the PdPt catalysts studied (inset of Fig. 3b). This is in agreement with previous studies of O<sub>2</sub> reduction on Pd and Pt catalysts in acid media [11,18,25-27].

For better comparison of the RDE results the  $j$ - $E$  curves of ORR recorded at 1900 rpm are shown in Fig. 3c. Half-wave potentials ( $E_{1/2}$ ) of oxygen reduction for all the alloyed catalysts were higher than that of Pd nanocubes and were comparable to that of cubic Pt nanoparticles (Table 1). The onset potential for Pd<sub>36</sub>Pt<sub>64</sub> was the highest.

Tafel plots were constructed from the RDE data on O<sub>2</sub> reduction at 1900 rpm as shown in Fig. 3d. Two regions with distinct slope values were observed (Table 1). In the low overpotential region the slope was close to -60 mV and the rate-determining step of oxygen reduction on oxide-covered PdPt alloys is the first electron transfer. At high overpotentials the Tafel slope value was over -130 mV, which is slightly higher than that reported for Pd and Pt electrodes in early work [25,28]. Similar slope values have been found for different Pd- and Pt-based catalysts [18,26,27,29,30].

The reduction of oxygen on Pd and Pt is a structure-sensitive reaction and the ORR activity depends on the strength of adsorption of the structure-sensitive electrolyte species on the ( $hkl$ ) facets. It has been demonstrated that the electrocatalytic activity for ORR on Pt( $hkl$ ) monocrystals in H<sub>2</sub>SO<sub>4</sub> solution decreases in the following order: Pt(110) > Pt(100) > Pt(111) [28,31,32]. For Pd monocrystals the ORR activity dependence on the facets in HClO<sub>4</sub> solution was found to increase as follows: Pd(110) < Pd(111) < Pd(100) [33]. The ORR studies on Pd

nanocubes have shown enhanced activity towards  $O_2$  reduction in sulphuric acid solution, which has been attributed to the predominance of Pd(100) facets on nanocubes [18,29]. Availability of very small amount of (110) sites on the PdPt alloy nanocube surface might cause a slight change in the catalyst activity in acid electrolyte. The specific activity (SA) of  $O_2$  reduction at 0.9 V was calculated from the kinetic current ( $I_k$ ) normalised to the real surface area. The SA values are given in Table 1. The specific activity of Pd<sub>36</sub>Pt<sub>64</sub> was higher than that of Pd nanocubes, but still lower than that of Pt nanocubes. Hoshi et al. have shown that a Pt monolayer on Pd(100) decreases the activity [34]. On the other hand Pd-Pt nanodendrites with 85% of Pt had higher activity than that of Pt/C [9]. In this work the largest Pt content was 64% and it can be observed that SA starts to increase, but still does not surpass that of Pt nanocubes. It has been suggested that with higher Pt content the  $O_2$  adsorption is more favourable and thus increases the ORR activity [9]. Apparently, the lower activity of PdPt nanocubes is related to a decrease in the number of dual Pt-Pt sites as compared to monometallic Pt particles. Another reason for lower SA value of PdPt nanocubes might be the adsorption of anions on the metal that is competing with  $O_2$  adsorption. Further work is ongoing to study the ORR kinetics on these PdPt alloy nanocubes in alkaline media.

#### 4. Conclusions

PdPt alloy nanocubes synthesised in this work showed enhanced electrocatalytic activity towards the ORR compared to Pd nanocubes. TEM images showed that PdPt nanoparticles were cubic-shaped. From EDX measurements the composition of Pd and Pt metals in the alloys was determined. The electroreduction of oxygen proceeded via four-electron pathway on all the electrocatalysts studied. The Tafel analysis revealed that the mechanism of  $O_2$  reduction on PdPt alloy nanocubes is similar to that of Pd and Pt cubic nanoparticles.



**Acknowledgements**

This research was financially supported by institutional research funding (IUT20-16) of the Estonian Ministry of Education and Research and by the Estonian Research Council (Grant No. 9323). KJ thanks the Archimedes Foundation for scholarship. JMF acknowledges financial support from MINECO (Spain), project CTQ2013-44083-P.

**References**

- [1] I. Katsounaros, S. Cherevko, A.R. Zeradjanin, K.J.J. Mayrhofer, Oxygen electrochemistry as a cornerstone for sustainable energy conversion, *Angew. Chem. Int. Ed.* 53 (2014) 102-121.
- [2] H.A. Gasteiger, S.S. Kocha, B. Sompalli, F.T. Wagner, Activity benchmarks and requirements for Pt, Pt-alloy, and non-Pt oxygen reduction catalysts for PEMFCs, *Appl. Catal. B: Environ.* 56 (2005) 9-35.
- [3] J.W. Hong, S.W. Kang, B.-S. Choi, D. Kim, S.B. Lee, S.W. Han, Controlled synthesis of Pd-Pt alloy hollow nanostructures with enhanced catalytic activities for oxygen reduction, *ASC Nano* 6 (2012) 2410-2419.
- [4] E. Antolini, Palladium in fuel cell catalysis, *Energy Environ. Sci.* 2 (2009) 915-931.
- [5] F.J. Vidal-Iglesias, A. López-Cudero, J. Solla-Gullón, A. Aldaz, J.M. Feliu, Pd-modified shape-controlled Pt nanoparticles towards formic acid electrooxidation, *Electrocatalysis* 3 (2012) 313-323.
- [6] C. Kim, J. Kim, S. Yang, H. Lee, One-pot synthesis of Pd@PdPt core-shell nanocubes on carbon supports, *RSC Adv.* 4 (2014) 63677-63680.
- [7] Z.-C. Zhang, J.-F. Hui, Z.-G. Guo, Q.-Y. Yu, B. Xu, X. Zhang, Z.-C. Liu, C.-M. Xu, J.-S. Gao, X. Wang, Solvothermal synthesis of Pt-Pd alloys with selective shapes and their enhanced electrocatalytic activities, *Nanoscale* 4 (2012) 2633-2639.
- [8] J. Wu, A. Gross, H. Yang, Shape and composition-controlled platinum alloy nanocrystals using carbon monoxide as reducing agent, *Nano Lett.* 11 (2011) 798-802.
- [9] B. Lim, M. Jiang, P.H.C. Camargo, E.C. Cho, J. Tao, X. Lu, Y. Zhu, Y. Xia, Pd-Pt bimetallic nanodendrites with high activity for oxygen reduction, *Science* 324 (2009) 1302-1305.

- [10] K. Gong, M.B. Vukmirovic, C. Ma, Y. Zhu, R.R. Adzic, Synthesis and catalytic activity of Pt monolayer on Pd tetrahedral nanocrystals with CO-adsorption-induced removal of surfactants, *J. Electroanal. Chem.* 662 (2011) 213-218.
- [11] J.-N. Zheng, L.-L. He, F.-Y. Chen, A.-J. Wang, M.-W. Xue, J.-J. Feng, Simple one-pot synthesis of platinum-palladium nanoflowers with enhanced catalytic activity and methanol-tolerance for oxygen reduction in acid media, *Electrochim. Acta* 137 (2014) 431-438.
- [12] J.-J. Lv, J.-N. Zheng, L.-L. Chen, M. Lin, A.-J. Wang, J.-R. Chen, J.-J. Feng, Facile synthesis of bimetallic alloyed Pt-Pd nanocubes on reduced graphene oxide with enhanced electrocatalytic properties, *Electrochim. Acta* 143 (2014) 36-43.
- [13] Y. Lu, Y. Jiang, W. Chen, Graphene nanosheet-tailored PtPd concave nanocubes with enhanced electrocatalytic activity and durability for methanol oxidation, *Nanoscale* 6 (2014) 3309-3315.
- [14] C.-L. Lee, C.-C. Yang, C.-R. Liu, Z.-T. Liu, J.-S. Ye, Pt-coated Pd nanocubes as catalysts for alkaline oxygen reduction activity, *J. Power Sources* 268 (2014) 712-717.
- [15] M. Shao, G. He, A. Peles, J.H. Odell, J. Zeng, D. Su, J. Tao, T. Yu, Y. Zhu, Y. Xia, Manipulating the oxygen reduction activity of platinum shells with shape-controlled palladium nanocrystal cores, *Chem. Commun.* 49 (2013) 9030-9032.
- [16] X. Huang, Y. Li, Y. Li, H. Zhou, X. Duan, Synthesis of PtPd bimetal nanocrystals with controllable shape, composition, and their tunable catalytic properties, *Nano Lett.* 12 (2012) 4265-4270.
- [17] W. Niu, Z.-Y. Li, L. Shi, X. Liu, H. Li, S. Han, J. Chen, G. Xu, Seed-mediated growth of nearly monodisperse palladium nanocubes with controllable sizes, *Cryst. Growth Des.* 8 (2008) 4440-4444.

- [18] H. Erikson, A. Sarapuu, K. Tammeveski, J. Solla-Gullón, J.M. Feliu, Enhanced electrocatalytic activity of cubic Pd nanoparticles towards the oxygen reduction reaction in acid media, *Electrochem. Commun.* 13 (2011) 734-737.
- [19] R.A. Martínez-Rodríguez, F.J. Vidal-Iglesias, J. Solla-Gullón, C.R. Cabrera, J.M. Feliu, Synthesis of Pt nanoparticles in water-in-oil microemulsion: effect of HCl on their surface structure, *J. Am. Chem. Soc.* 136 (2014) 1280-1283.
- [20] J. Solla-Gullón, A. Rodes, V. Montiel, A. Aldaz, J. Clavilier, Electrochemical characterisation of platinum-palladium nanoparticles prepared in a water-in-oil microemulsion, *J. Electroanal. Chem.* 554-555 (2003) 273-284.
- [21] R. Woods, in: A.J. Bard (Ed.), *Electroanalytical Chemistry*, vol. 9, Marcel Dekker, New York, 1976, pp. 1-162.
- [22] A.J. Bard, L.R. Faulkner, *Electrochemical Methods*, 2nd ed., Wiley, New York, 2001.
- [23] S. Gottesfeld, I.D. Raistrick, S. Srinivasan, Oxygen reduction kinetics on a platinum RDE coated with a recast Nafion film, *J. Electrochem. Soc.* 134 (1987) 1455-1462.
- [24] D.R. Lide (Ed.), *CRC Handbook of Chemistry and Physics*, 82nd ed., CRC Press, Boca Raton, 2001.
- [25] N. Alexeyeva, A. Sarapuu, K. Tammeveski, F.J. Vidal-Iglesias, J. Solla-Gullón, J.M. Feliu, Electroreduction of oxygen on Vulcan carbon supported Pd nanoparticles and Pd-M nanoalloys in acid and alkaline solutions, *Electrochim. Acta* 56 (2011) 6702-6708.
- [26] K. Jukk, N. Alexeyeva, C. Johans, K. Kontturi, K. Tammeveski, Oxygen reduction on Pd nanoparticle/multi-walled carbon nanotube composites, *J. Electroanal. Chem.* 666 (2012) 67-75.
- [27] K. Jukk, J. Kozlova, P. Ritslaid, V. Sammelselg, N. Alexeyeva, K. Tammeveski, Sputter-deposited Pt nanoparticle/multi-walled carbon nanotube composite catalyst for oxygen reduction reaction, *J. Electroanal. Chem.* 708 (2013) 31-38.

- [28] N.M. Markovic, H.A. Gasteiger, P.N. Ross, Oxygen reduction on platinum low-index single-crystal surfaces in sulfuric acid solution: rotating ring – Pt(*hkl*) disk studies, *J. Phys. Chem.* 99 (1995) 3411.
- [29] H. Erikson, A. Sarapu, N. Alexeyeva, K. Tammeveski, J. Solla-Gullón, J.M. Feliu, Electrochemical reduction of oxygen on palladium nanocubes in acid and alkaline solutions, *Electrochim. Acta* 59 (2012) 329-335.
- [30] K. Jukk, N. Alexeyeva, A. Sarapu, P. Ritslaid, J. Kozlova, V. Sammelselg, K. Tammeveski, Electroreduction of oxygen on sputter-deposited Pd nanolayers on multi-walled carbon nanotubes, *Int. J. Hydrogen Energy* 38 (2013) 3614-3620.
- [31] M.D. Maciá, J.M. Campiña, E. Herrero, J.M. Feliu, On the kinetics of oxygen reduction on platinum stepped surfaces in acidic media, *J. Electroanal. Chem.* 564 (2004) 141-150.
- [32] A. Kuzume, E. Herrero, J.M. Feliu, Oxygen reduction on stepped platinum surfaces in acidic media, *J. Electroanal. Chem.* 599 (2007) 333-343.
- [33] S. Kondo, M. Nakamura, N. Maki, N. Hoshi, Active sites for the oxygen reduction on the low and high index planes of palladium, *J. Phys. Chem. C* 113 (2009) 12625-12628.
- [34] N. Hoshi, M. Nakamura, S. Kondo, Oxygen reduction on the low index planes of palladium electrodes modified with a monolayer of platinum film, *Electrochem. Commun.* 11 (2009) 2282-2284.

**Figure captions**

**Figure 1.** TEM images of PdPt catalysts: (a) Pd<sub>36</sub>Pt<sub>64</sub>, (b) Pd<sub>54</sub>Pt<sub>46</sub> and (c) Pd<sub>72</sub>Pt<sub>28</sub>. Size distribution of the catalysts is shown in Fig. (d).

**Figure 2.** (a) Electro-oxidation of pre-adsorbed CO and (b) cyclic voltammograms after CO-oxidation on PdPt catalysts in Ar-saturated 0.5 M H<sub>2</sub>SO<sub>4</sub>. (a)  $\nu = 20 \text{ mV s}^{-1}$  and (b)  $50 \text{ mV s}^{-1}$ . Current densities are normalised to the real surface area of electrocatalysts.

**Figure 3.** (a) RDE voltammetry curves for oxygen reduction on Pd<sub>54</sub>Pt<sub>46</sub> alloy nanocubes in O<sub>2</sub>-saturated 0.5 M H<sub>2</sub>SO<sub>4</sub> ( $\nu = 10 \text{ mV s}^{-1}$ ), (b) K-L plots for ORR in 0.5 M H<sub>2</sub>SO<sub>4</sub> (inset shows the potential dependence of  $n$ ), (c) comparison of the RDE results for the ORR ( $\nu = 10 \text{ mV s}^{-1}$ ,  $\omega = 1900 \text{ rpm}$ ) and (d) Tafel plots for ORR in 0.5 M H<sub>2</sub>SO<sub>4</sub> ( $\omega = 1900 \text{ rpm}$ ). Current densities are normalised to the geometric area of GC.

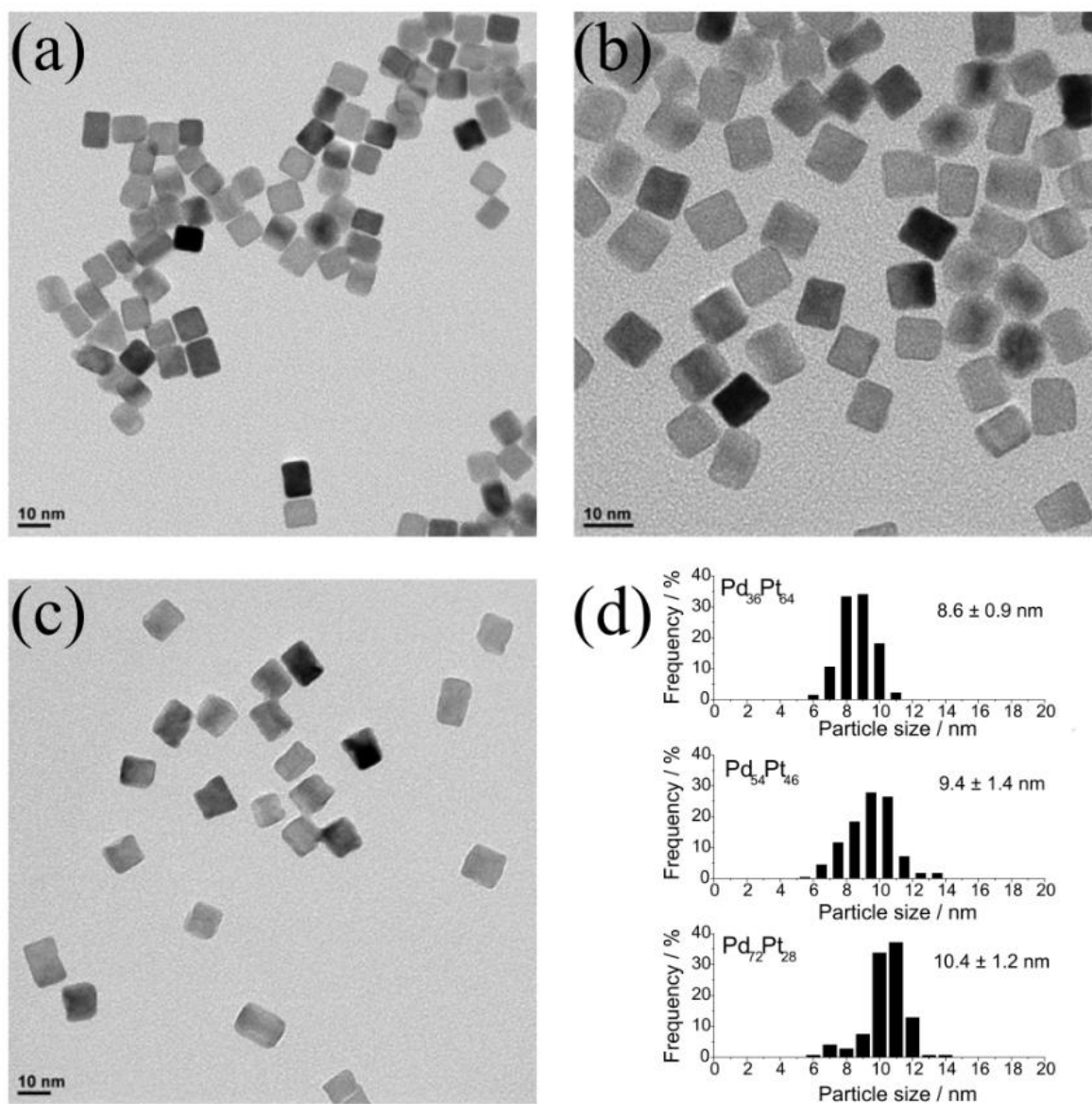


Figure 1

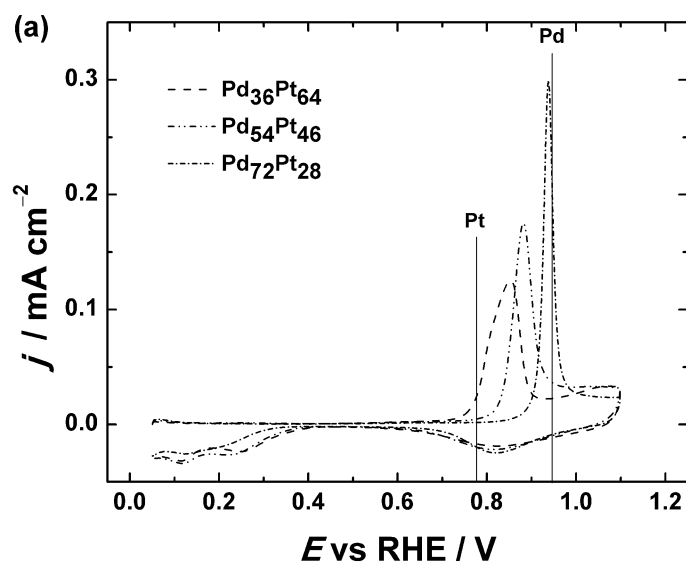


Figure 2a



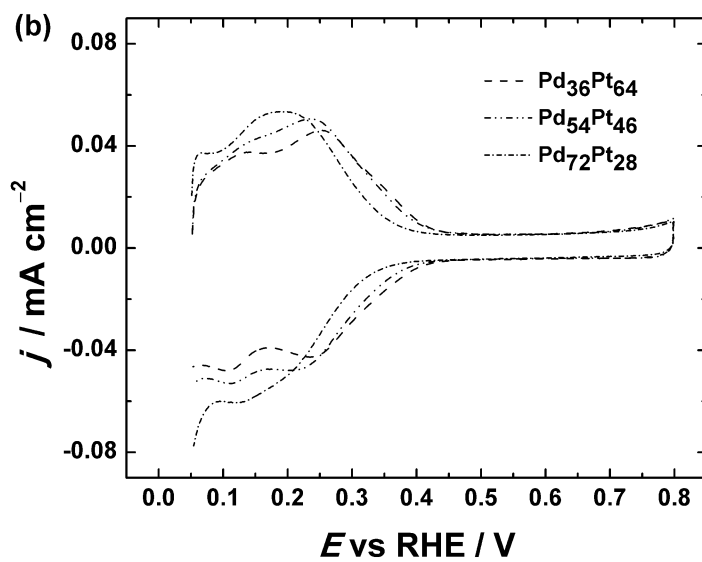


Figure 2b

ACCEPTED

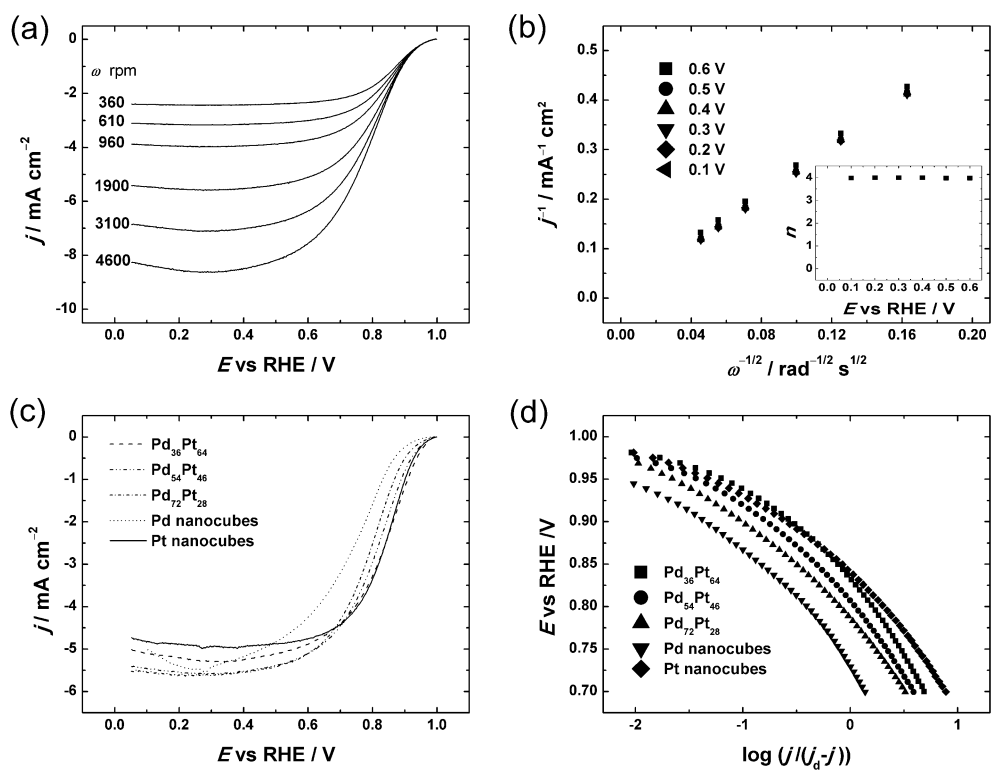
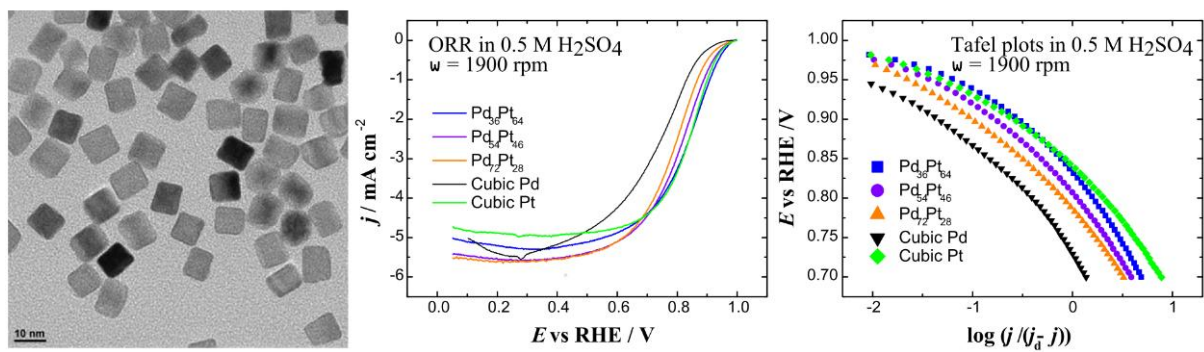


Figure 3



Graphical abstract

**Table 1.** Kinetic parameters for oxygen reduction on PdPt nanocubes, cubic Pd and cubic Pt in O<sub>2</sub>-saturated 0.5 M H<sub>2</sub>SO<sub>4</sub>,  $\omega = 1900$  rpm.

Electrode	$A_r$ (cm <sup>2</sup> )	Tafel slope (mV)		$E_{1/2}$ (V)	SA at 0.9 V (mA cm <sup>-2</sup> )
		I region*	II region*		
Pd <sub>36</sub> Pt <sub>64</sub>	0.99	-62	-151	0.83	0.089
Pd <sub>54</sub> Pt <sub>46</sub>	0.89	-62	-152	0.81	0.072
Pd <sub>72</sub> Pt <sub>28</sub>	0.55	-66	-136	0.79	0.070
Pd nanocubes	0.46	-64	-134	0.73	0.078
Pt nanocubes	0.75	-58	-142	0.84	0.113

\* Region I corresponds to low current densities and Region II to high current densities.

**Research highlights**

- PdPt alloy nanocubes were synthesised in the presence of polyvinylpyrrolidone (PVP)
- PVP was removed from PdPt surface by centrifugation and CO adsorption and oxidation
- PdPt nanocubes were used as catalysts for oxygen reduction reaction in 0.5 M H<sub>2</sub>SO<sub>4</sub>
- The alloyed PdPt catalysts showed an enhanced electrocatalytic activity for ORR
- The electroreduction of oxygen proceeded via 4-electron pathway on PdPt catalysts

ACCEPTED MANUSCRIPT